



Electromagnetic Properties of $\text{Mg}_{0.6}\text{Ni}_{0.4}\text{Al}_{0.1}\text{Fe}_{1.9}\text{O}_4$ -Graphene Oxide Nanocomposites

Fariha Nasrullah¹ · M. U. Islam¹ · Aamir Nazir¹ · Shahzad Naseem²

Received: 23 February 2022 / Accepted: 13 June 2022 / Published online: 24 June 2022
© The Author(s), under exclusive licence to Springer Science+Business Media, LLC, part of Springer Nature 2022

Abstract

The current report elaborates on the fabrication and evaluation of magnetic and electrical properties of technologically beneficial composites of spinel ferrite and graphene oxide. The synthesis of spinel ferrite with composition $\text{Mg}_{0.6}\text{Ni}_{0.4}\text{Al}_{0.1}\text{Fe}_{1.9}\text{O}_4$ is done by using the sol–gel auto combustion technique. Modified Hummers method is adopted for the preparation of graphene oxide. The nanocomposites of spinel ferrite-GO (C_1 , C_2 , C_3) with appropriate ratios of GO are fabricated by sonication of GO and ferrite in water. XRD patterns confirmed the successful synthesis of single-phase cubic ferrite and GO. The dielectric constant of all the prepared samples decreased with increasing the applied frequency, obeying Maxwell–Wagner model. The decrease in temperature-dependent resistivity with increasing temperature indicates semiconducting nature of all samples. The M-H loops of all samples are narrow. The squareness ratio of all the samples is less than 1, which suggests that the present investigated samples are multi-domain. The sample C_1 (90% ferrite, 10% GO) with high saturation magnetization, high coercivity, low dielectric constant, and high resistivity made it suitable for use in high-frequency applications like microwave absorbers.

Keywords Ferrite · Graphene oxide · Nanocomposites · Magnetic properties · Electrical properties

1 Introduction

Graphene and graphene composites are vital materials nowadays due to versatile properties of graphene. Graphene consists of only carbon atoms bonded together in a single-layered sheet with a honeycomb arrangement of the lattice [1]. Graphene is a 2D layer allotrope of sp^2 hybridized carbon atoms. The sp^2 hybridization between one s-orbital and two p-orbitals leads to a trigonal planar structure with the formation of a σ -bond between carbon atoms with a separation of 1.42 Å [2]. Graphene possesses startling properties, e.g., intrinsic flexibility, excellent optical transparency, large electrical and thermal conductivity high charge mobility greater than Si, and the large specific area, the ultra-high surface-to-volume ratio. Graphene-based nanomaterials (GBNS) can be classified depending upon the number of layers stacked. When GBNS is in the oxidized state, the structure can be classified into two types, graphene

oxide (GO) and reduced graphene oxide (rGO) [3–5]. The vital functional groups of GO are alcohols and epoxides whereas ketone groups lie in the corners. Hydroxyl (–OH), carbonyl (–CO¹/₄), carboxyl (–COOH), and epoxide (–O–) are the four functional groups in graphene oxide [6]. Magnetic functionalization of carbon materials with magnetic particles reveals novel GO/magnetic composite materials for high-frequency applications and EMI shielding [3, 7]. It is reported that the Mg-ferrite/GO composites exhibit high adsorption abilities for organic pollutants [8, 9]. Magnesium ferrite is considered to be the most suitable material for microwave absorbing materials due to its high resistivity and low dielectric loss. Its magnetic and electrical properties may be enhanced by substituting transition metal cations [10, 11]. The present study aims to synthesize and characterize $\text{Mg}_{0.6}\text{Ni}_{0.4}\text{Al}_{0.1}\text{Fe}_{1.9}\text{O}_4$ and Mg ferrite/GO nanocomposites for high-frequency applications.

1.1 Experimental Procedure

1.1.1 Preparation of Spinel Ferrites

Synthesis of spinel ferrite is accompanied by the sol–gel method. Chemicals used for the preparation of the sample were magnesium nitrate, nickel nitrate, aluminum nitrate,

✉ M. U. Islam
dr.misbahulislam@bzu.edu.pk

¹ Department of Physics, Bahauddin Zakariya University, Multan, Pakistan

² Center of Excellence in Solid State Physics, Punjab University, Lahore, Pakistan

iron nitrate, and citric acid. All the chemicals were taken in stoichiometric amounts and dissolved in 100 ml deionized water separately. All these solutions were poured down in a 500-ml beaker and stirred for 20–30 min on a hot plate for making a homogeneous solution. Drops of ammonium hydroxide were added to the solution to neutralize it. The solution was heated with continuous stirring to maintain the temperature of the solution at 60–80°. With continuous stirring and heating, the solution was first converted into a colloidal solution and then finally into a gel. After the formation of gel, the stirring is stopped and heated to 300 °C to convert the gel into ashes. This ash was ground and then sintered at 900 °C for 5 h to get a fine powder.

1.1.2 Preparation of Graphene Oxide by Hummer's Method

Graphene oxide will be prepared by Hummer's method [12]. An appropriate amount of graphite powder was added to a 1000-ml beaker. The solution was continuously stirred for 1 h. After that, 2 g of NaNO₃ was added to the solution and stirring continued for a couple of hours. Then, the beaker was removed from the stirrer and placed in a tub filled with ice cubes to cool down the solution up to 5°C. The beaker was again placed on a stirrer. KMnO₄ (12 g) was added slowly within 2 h. After adding a small number of KMnO₄ (2 g), the sample was continuously stirred for 3 to 5 min and then removed from the stirrer and again placed in an ice tub to keep the sample cool due to exothermic reaction. After adding KMnO₄ completely, the temperature of the stirrer was set between 25 and 35 °C, and 250 ml deionized water was added to the sample solution. The sample was continuously stirred for 3 to 5 h for complete oxidation. In the last step, the reaction was terminated by adding 10 ml of hydrogen peroxide and the sample solution was stirred for half-hour. Here, the reaction was completed and GO was in solution form. The solution was centrifuged to remove impurities. Finally, the paste of GO was dried at 80° for 4–5 h and ground to get a fine powder.

1.1.3 Composites Preparation

The weighed amount of ferrite and GO samples were transferred into three different beakers of 100 ml, labeled as C₁, C₂, C₃. Ethanol was taken as a solvent in these three beakers separately. Then, these beakers were placed in the sonicator for 20 min at room temperature. These samples were poured into the pattery dishes and kept in a drying

oven for 3 h at 60 °C for drying the composites and after grinding the dried samples, the final product (fine powder) is prepared.

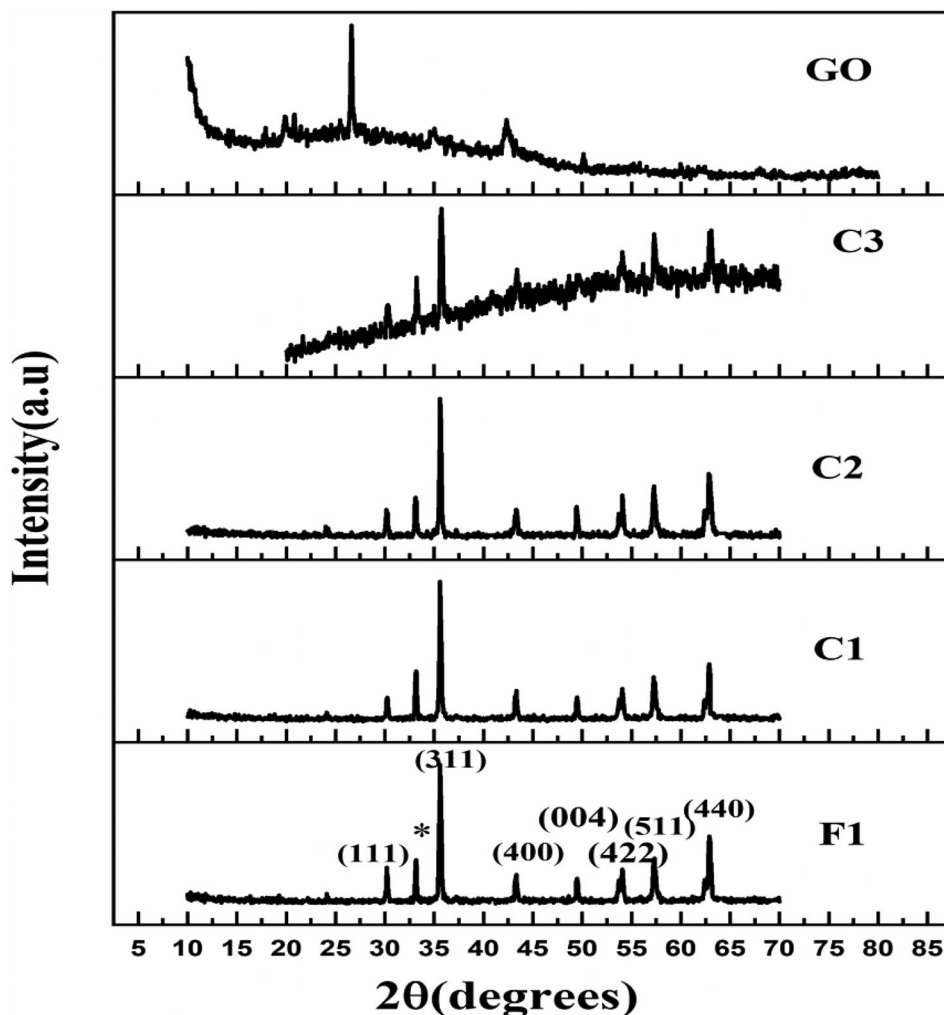
2 Results and Discussions

The XRD patterns of Mg_{0.6}Ni_{0.4}Al_{0.1}Fe_{1.9}O₄, graphene oxide, and their composites are shown in Fig. 1 The characteristic reflections of spinel ferrite were observed at 30.30°, 33.24°, 35.70°, 43.40°, 54.03°, 57.32°, 62.97° with respective hkl's (111), (311), (400), (422), (511), and (400) are observed in X-ray spectrum. Single-phase spinel ferrite is obtained, which belongs to space group Fd3m. An additional peak at 33.242° also appeared, which indicates the presence of α-Fe₂O₃ [14, 15]. The XRD pattern of GO shows the characteristic peaks at 2θ = 10.11° with interlayer spacing $d = 0.89$ nm, at 2θ = 26.61°, and at 43° which confirms the formation of graphene oxide. The peaks of GO depend on the level of oxidation. As the oxidation level increases, the rest of the peaks disappears except 2θ = 10–11° [13]. The main peaks of pure ferrite sample and GO appeared in XRD spectra of all composites indicating their successful synthesis [16]. The suppression of GO characteristic peaks in the composites C₁, C₂, and C₃ is an indication of exfoliation in spinel ferrite between interlayers of GO sheets. The variation in d -values also confirmed the exfoliation of GO (Table 1).

2.1 Electrical Resistivity

Keithly source meter model 2400 is used to measure the DC resistivity. From Fig. 2, it is noted that at room temperature, the conductivity of GO is higher than ferrite particles. The electrical properties of graphene oxide are based on its oxidation level. The sp²/sp³ ratio has a direct impact on oxidation levels. The sp²/sp³ ratio can be varied by reduction or addition of oxygen functionalized groups in GO's structure. In this way, the electrical properties of GO can be tuned. The ferrite particles are expected to enter into a hexagonal honey comb-like structure that results in a slight increment in resistivity. Further by increasing the GO content and decreasing the ferrite content, the number of GO charge carriers contributing to the conduction mechanism is increased and the number of ferrite particles that occupy the honeycomb structure of GO is decreased, resulting in an increase in density of GO charges as well as conduction mechanism. Ultimately, the resistivity decreased. The

Fig. 1 X-ray diffraction pattern of pure spinel ferrite F1, C1, C2, C3, and GO (* represents $\alpha\text{Fe}_2\text{O}_3$)



hopping mechanism is supported by the enhanced charge contents of GO [17].

Figure 3 shows the Arrhenius plots of the samples C_1 , C_2 , and C_3 . It is observed that the resistivity of all investigated samples decreases by increasing temperature,

which is an indication of semiconducting behavior. Figure 4 shows the activation energy vs GO content. It is observed that the activation energy is decreased as GO

Table 1 Diffraction angles, d -values, and hkl s for $\text{Mg}_{0.6}\text{Ni}_{0.4}\text{Al}_{0.1}\text{Fe}_{1.9}\text{O}_4$ spinel ferrite

2θ (degrees)	d (Å)	hkl
30.30	2.949	(111)
33.24	2.695	$\alpha\text{-Fe}_2\text{O}_3$
35.70	2.515	(311)
43.40	2.085	(400)
54.03	1.697	(422)
57.32	1.607	(511)
62.97	1.474	(440)
Diffraction angles, d -values, and hkl s for graphene oxide (GO)		
10.11	8.9	(001)
26.61	1.7	(002)
43	1.1	(004)

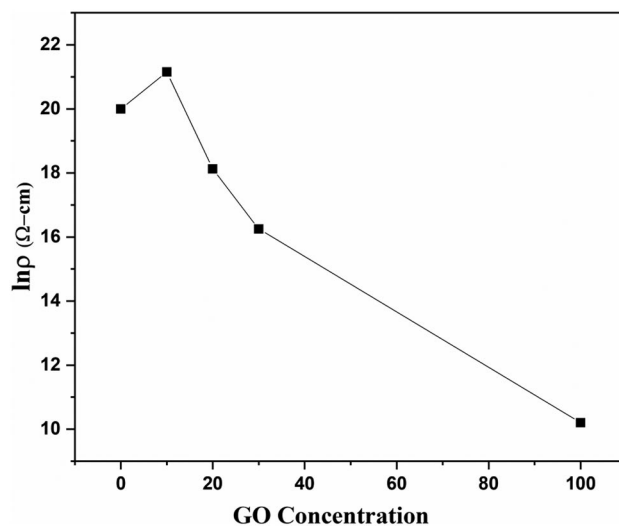
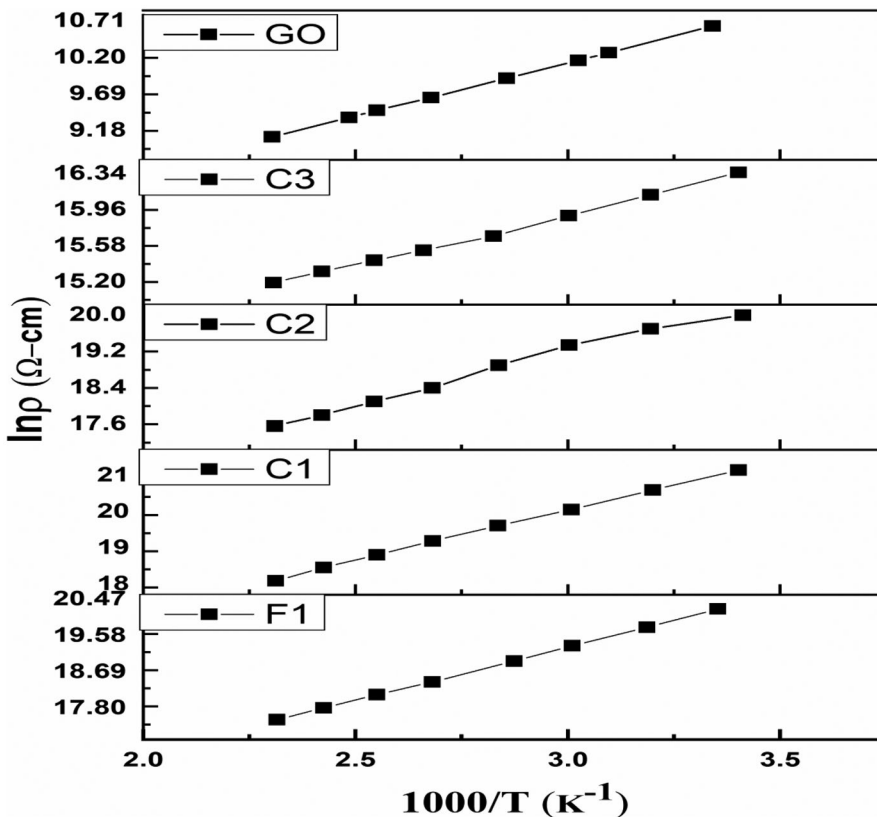


Fig. 2 Variation of dc resistivity vs GO concentration for pure spinel ferrite F1, C1, C2, C3, and GO

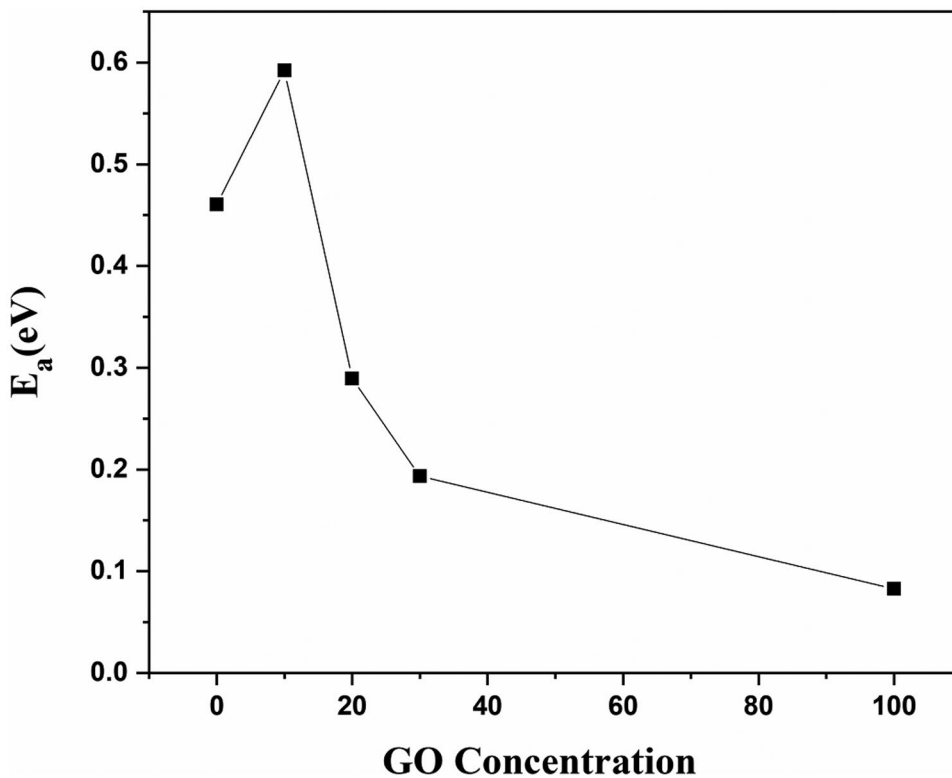
Fig. 3 Arrhenius plots for pure spinel ferrite F1, composites C1, C2, C3, and GO



is substituted. The activation energy follows the resistivity versus GO contents. It is noted that the greater the resistivity of the sample, the higher will be its activation

energy and vice versa [18], whereas the resistivity of GO depends on the level of oxidation and hopping of charges.

Fig. 4 Variation of activation energy vs GO concentration for pure spinel ferrite F1, C1, C2, C3, and GO



2.2 Dielectric Properties

Frequency-dependent dielectric properties of $Mg_{0.6}Ni_{0.4}Al_{0.1}Fe_{1.9}O_4$, GO and their ferrite/GO composites (with 10%Wt, 20%Wt, 30% wt of GO) are discussed below:

Figure 5 shows the dielectric constant vs frequency for all the samples. The graphs show the typical behavior of ferrites following the Maxwell–Wagner-type model [4]. It assumes a two-layered heterostructure of ferrites, that is, conducting grains, separated by highly resistive grain boundaries. The high value of ϵ' at low frequency is due to interfacial polarization and at intermediate high frequency, the dipoles exhibit dispersion and at further high frequency, the ϵ' is almost independent of frequency because the dipoles don't follow the applied frequency. From Fig. 5, it can be observed that the magnitude of the ϵ' increases as GO content increases. The GO content has a significant effect on the dielectric constant, and it increases the conduction due to the hopping of charge carriers (Fe^{2+} to $Fe^{3+} + e^-$). Figure 5 shows the increasing trend of ϵ' . The dielectric constant of samples is in the following trend: ϵ' of ferrite $< C_1 < C_2 < C_3 < GO$. The combined graph ϵ' vs frequency for all samples is shown in Fig. 5. If figures of the dielectric constant of samples are compared with Fig. 2 of room temperature resistivity, these two parameters ϵ' and ϵ'' behave oppositely. The values of $\sqrt{\rho}$. ϵ' for composites is constant as listed in Table 2 [17].

Figure 6 depicts the dielectric loss as a function of frequency for all the samples. The ϵ'' shows similar behavior

Table 2 Resistivity, dielectric constant and their product for $Mg_{0.6}Ni_{0.4}Al_{0.1}Fe_{1.9}O_4$ -GO composites

Composition	Resistivity (ρ) (Ohm-cm)	Dielectric constant (ϵ') at 10 kHz	$\sqrt{\rho} \times \epsilon'$
$Mg_{0.6}Ni_{0.4}Al_{0.1}Fe_{2-x}O_4$	3×10^8	3×10^3	5×10^7
$C_1=90\%$ FERRITE+ 10% GO	6×10^8	8×10^3	2×10^8
$C_2=80\%$ FERRITE+ 20% GO	6×10^7	2×10^4	1×10^8
$C_3=70\%$ FERRITE+ 30%GO	8×10^6	7×10^4	2×10^8
GO	1×10^4	3×10^7	3×10^9

as that of ϵ' and follows Maxwell–Wagner model [4]. The magnitude of ϵ'' is lesser than ϵ' . The dielectric loss shows the loss of energy due to defects, voids, or dislocations in the sample whereas ϵ' shows the capability of a dielectric to store energy by weakening the internal electric field. Figure 6 shows the value of ϵ'' at 20 Hz that shows the increasing value of ϵ'' from ferrite with the lowest value and GO with the highest value. Figure 6 shows the stacked graph of ϵ'' vs frequency for all prepared samples. The dielectric loss is found to decrease with the increasing concentration of GO. The addition of GO in spinel ferrite caused a decrease in electrical conductivity; this decrease in electronic conduction may be due to fact

Fig. 5 Dielectric constant vs frequency for composites C1, C2, C3

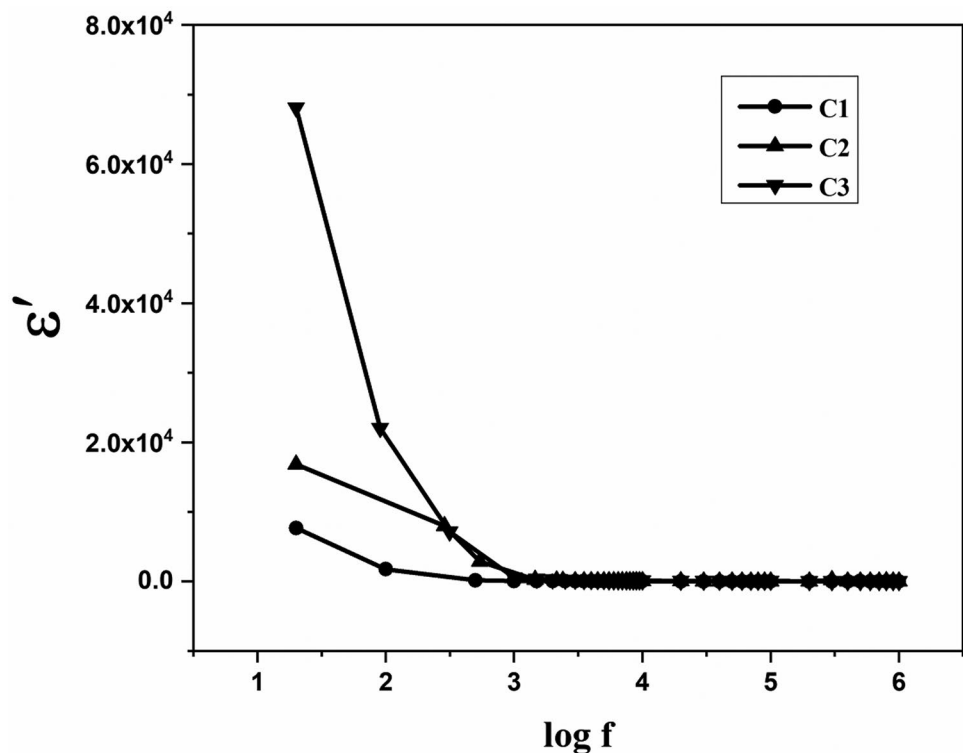
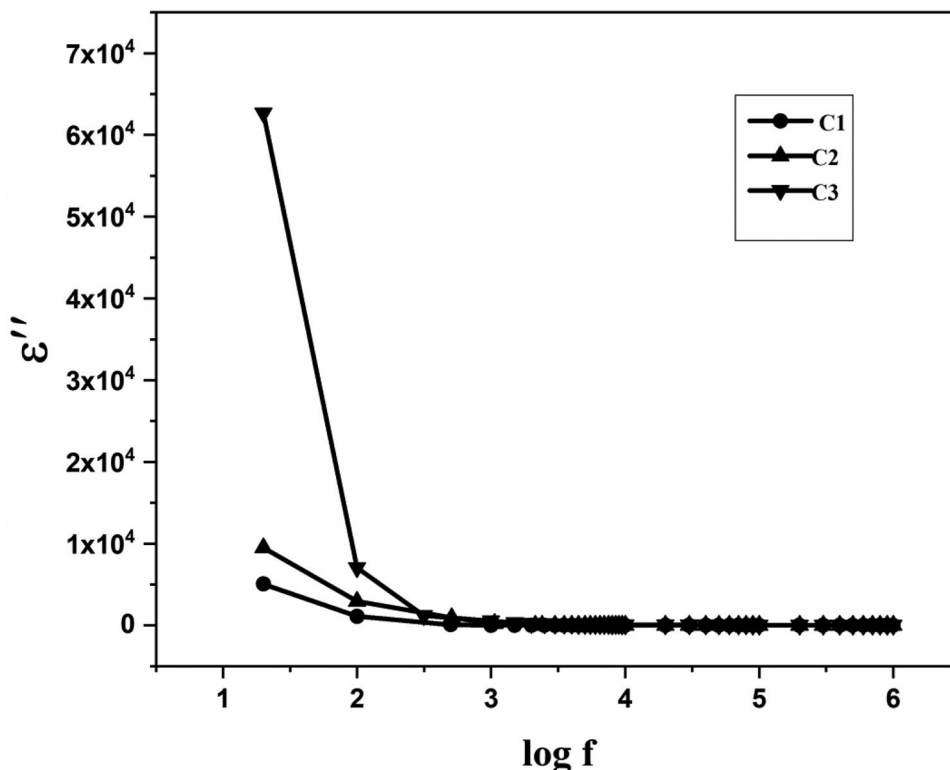


Fig. 6 Dielectric loss vs frequency for composites C1, C2, C3



that the defect sites created on pure graphene oxide might have been occupied by spinel ferrite and they effectively block the electron hopping [19]. The conductivity of GO is larger than pure ferrite. By increasing GO concentration in ferrite, the conductivity of composites increases due to an increase in charge content taking part in the hopping mechanism.

Figure 7 depicts ac conductivity vs frequency for ferrite, C₁, C₂, C₃, and GO respectively. At low-frequency values, the functional groups of GO supported enhanced

conduction. At an elevated frequency range, the charge carriers become active and actively support the conduction mechanism. But in the intermediate high-frequency range, the charge carriers at functional groups do not follow the applied frequency leading to a reduction in ac conductivity [20]. The conductivity of GO is larger than pure ferrite. By increasing GO concentration in ferrite, the conductivity of composites increases due to an increase in charge content taking part in the hopping mechanism.

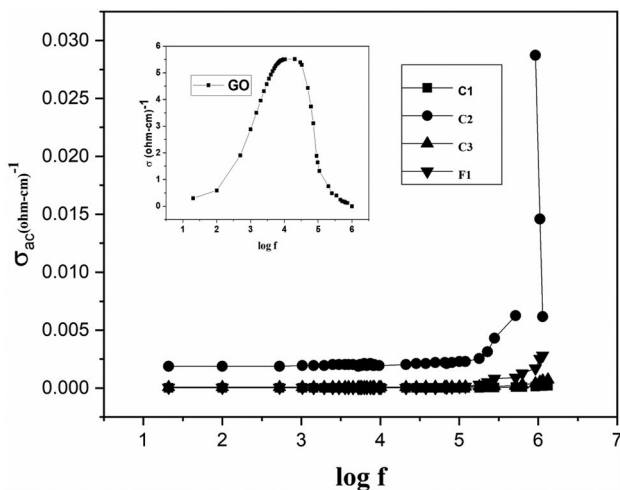
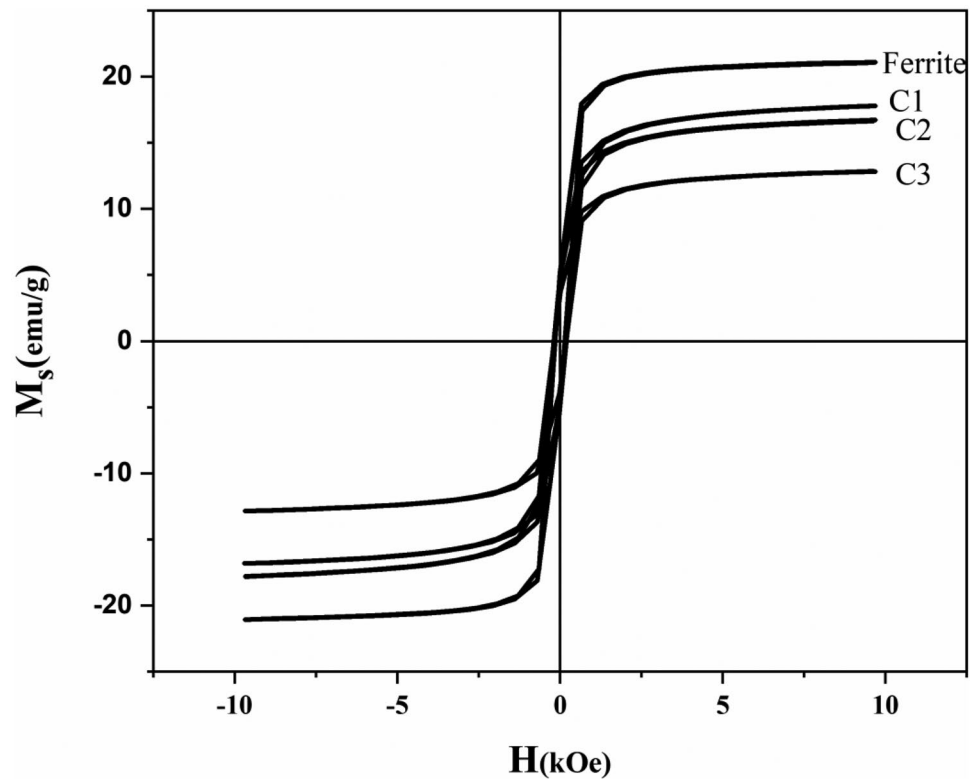


Fig. 7 Variation of ac conductivity vs log f for GO, F1, C1, C2, C3

2.3 Magnetic Properties

Figure 8 shows the M-H loops of Mg_{0.6}Ni_{0.4}Al_{0.1}Fe_{1.9}O₄, GO, and Mg-Ferrite/GO nanocomposites C₁, C₂, C₃ with a different weight percentage of ferrite and GO. M-H loops of all samples are shown in Fig. 8. The addition of GO content affects the M_s , M_r , and H_C values of pure ferrite. The saturation magnetization of pure ferrite is highest among all samples, which is 21.11 emu/g. By increasing the wt% of graphene oxide in composites, the M_s and M_r value decreases, as shown in Fig. 9. This is due to the non-collinear magnetic moment of surface spins. Another reason for a decrease in M_s value is that the magnetic moment of pure ferrite is greater than GO which resulted in weak A-B magnetic interaction between them [21, 22]. The remanence value of all samples is very small ranging from 0 to 5 emu/g. The squareness ratio is less than 1, which is indicative of

Fig. 8 M-H loops for ferrite, and composites C1, C2, and C3



single-domain samples. M_r vs GO concentration shows the same trend as that of M_s , as shown in Fig. 9. The M_r , M_s , and H_c values are listed in Table 3. Figure 10 shows coercivity vs GO content; it is observed that ferrite samples have the lowest coercivity value (146.73 Oe) and highest

average crystallite size (44.86 nm) among all prepared samples, whereas C_1 has the highest coercivity (186.71 Oe) and lowest average crystallite size (40.021 nm). C_2 and C_3 also follow the same trend as that of ferrite and C_1 [23]. The drastic increase in the coercivity values for composites as

Fig. 9 Saturation magnetization, M_s , and remanence, M_r , vs GO concentration for pure ferrite F1, and composites C1, C2, and C3

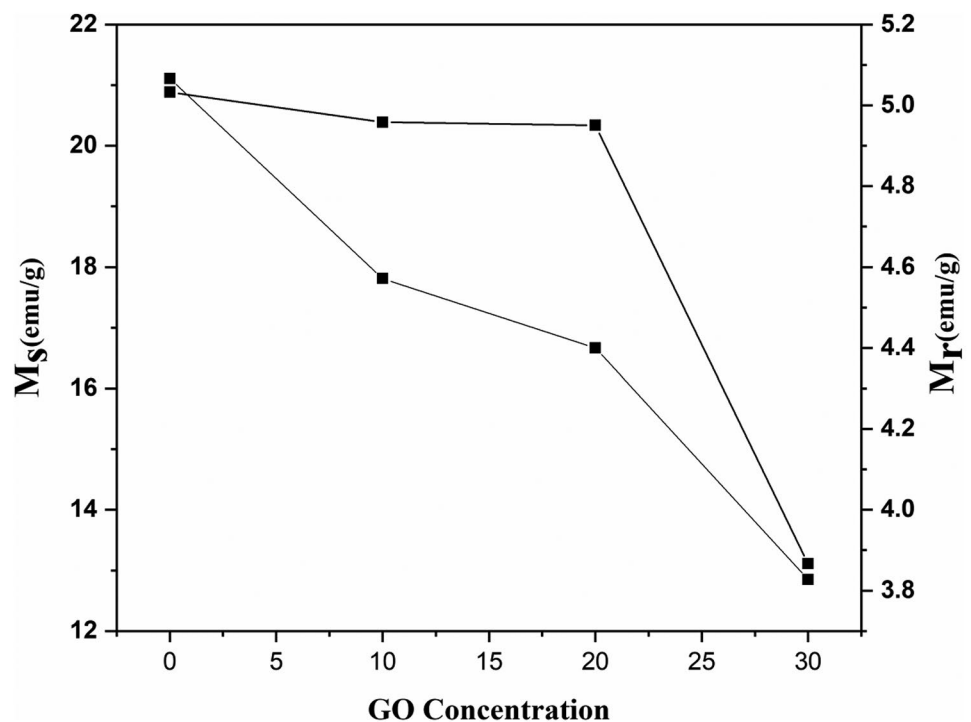
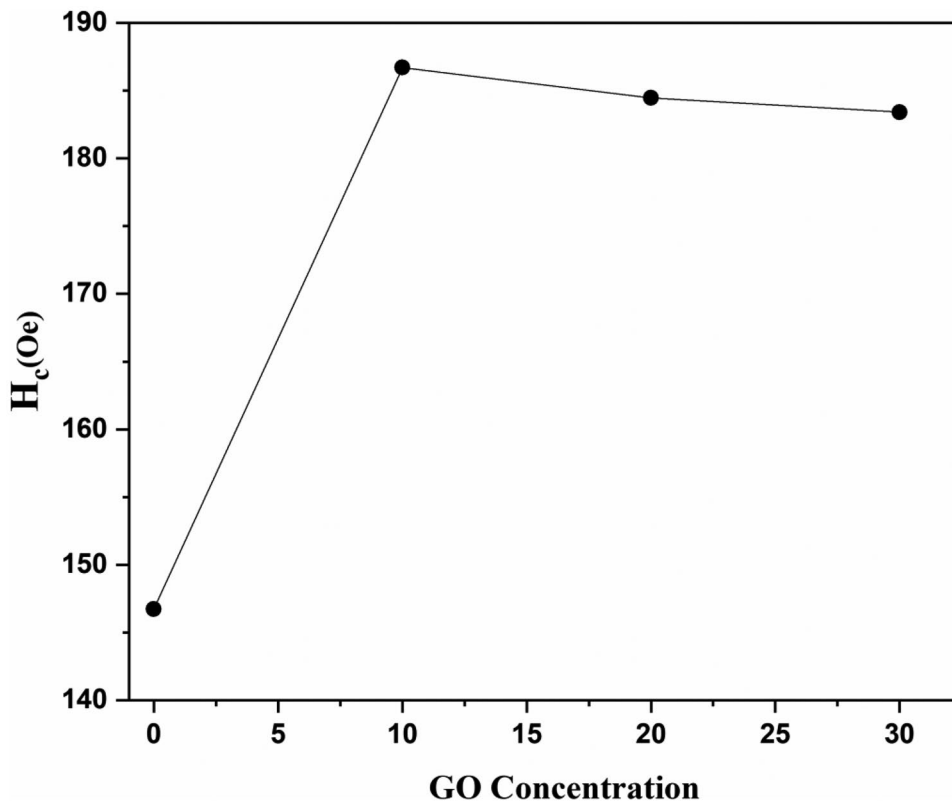


Table 3 Magnetic properties of $\text{Mg}_{0.6}\text{Ni}_{0.4}\text{Al}_{0.1}\text{Fe}_{1.9}\text{O}_4$ -GO composites

Composition	Saturation magnetization (M_s)	H_c (coercivity)	M_r (remanentivity)	M_r/M_s
$\text{Mg}_{0.6}\text{Ni}_{0.4}\text{Al}_{0.1}\text{Fe}_{1.9}\text{O}_4$	21.11 (emu/g)	146.73 (Oe)	5.03 (emu/g)	0.2383
$C_1=90\%$ FERRITE + 10% GO	17.80	186.71	4.95	0.2784
$C_2=80\%$ FERRITE + 20% GO	16.72	184.46	4.95	0.2961
$C_3=70\%$ FERRITE + 30% GO	12.83	183.41	3.86	0.3012

Fig. 10 Variation of Coercivity as a function of GO concentration for pure spinel ferrite F1, and composites C1, C2, C3

compared to ferrite samples may be due to a change in the microstructure of the composites where the possibility of defect formation is maximum on the graphene oxide sites. It is expected that domain wall pinning [24] may occur at these defect sites, thereby increasing coercivity.

3 Conclusions

The spinel ferrite $\text{Mg}_{0.6}\text{Ni}_{0.4}\text{Al}_{0.1}\text{Fe}_{1.9}\text{O}_4$ was synthesized by the sol-gel method and the Hummers method was used for preparing graphene oxide. XRD patterns revealed the formation of a single-phase cubic structure of spinel ferrite and successful synthesis of GO. The preparation of nanoparticles

was confirmed by crystallite size calculation by using the Sherrer formula which was in the range 31–48 nm. The observed value of room temperature electrical resistivity of spinel ferrite was $1.013 \times 10^6 \Omega\text{-cm}$. The observed ac conductivity of GO was higher than that of the ferrite sample which in turn decreased the resistivity value from 2.64×10^6 to $7.02 \times 10^3 \Omega\text{-cm}$ for C_1 to C_3 respectively. At 10-kHz frequency, the dielectric constant varies from 8×10^3 (C_1) to 7×10^4 (C_3) and dielectric loss ranges from 5×10^3 (C_1) to 6×10^4 (C_3). The saturation magnetization decreases from 17.8 (C_1) to 13 (C_3) emu/g due to weakening of AB interactions and coercivity decreases from 187 (C_1) to 184 (C_3) Oe due to defects in the composites. It is recommended that these samples may be used as microwave absorbing material.

Data Availability The raw/processed data required to reproduce these findings cannot be shared at this time as the data also forms part of an ongoing study.

References

1. Fatemeh, et al.: Recent developments in graphene and graphene oxide: properties, synthesis, and modifications: a review. *Chem. Select* **5**, 1–21 (2020)
2. Castro Neto, A.H., Guinea, F., Peres, N.M.R., Novoselov, K.S., Geim, A.K.: The electronic properties of graphene. *Rev. Modern Phys.* **81**(1), 109–162 (2009)
3. Durmus, Z., Durmus, A., Kavas, H.: Synthesis and characterization of structural and magnetic properties of graphene/hard ferrite nanocomposites as microwave-absorbing material. *J. Mater. Sci.* **50**, 1201–1213 (2015)
4. Ameer, S.: Iftikhar Hussain Gul, Nasir Mahmood, Muhammad Mujahid, Synthesis, characterization and optical properties of in situ ZnFe₂O₄ functionalized nano hybrids through modified solvothermal approach. *Opt. Mater.* **45**, 69–75 (2015)
5. Tan, T. L., Huang, J.: Carbon nanotubes and graphene (Second Edition). 341–374 (2014)
6. Nawaz, M., Islam, M. U., Aamir Nazir, M., Bano, I., Gul, I. H., Ajmal, M.: Transport properties in spinel ferrite/graphene oxide nanocomposites for electromagnetic shielding. *Ceram. Int.* **47**, 25505–25513 (2021)
7. Chung, D.D.L.: Materials for electromagnetic interference shielding. *Mater. Chem. Phys.* **255**, 123587 (2020)
8. Ateia, E.E., Mohammad, A.T., Elsayed, K.: Impact of Gd³⁺/graphene substitution on the physics properties of magnesium ferrite nanocomposites. *JMMM* **452**, 169–178 (2018). <https://doi.org/10.1016/j.jmmm.2017.12.053>
9. McAllister, M.J., et al.: Single sheet functionalized graphene by oxidation and thermal expansion of graphene. *Chem. Mater.* **19**, 4396–4404 (2007)
10. Kong, L.B., Li, Z. W., Lin, G. Q., Gan, Y. B.: Magneto – dielectric and magnetic properties of Mg- Co ferrite ceramics, electrical, dielectric, and magnetic properties, *J. Am. Ceram. Soc.* **90**, 2014–2112 (2007)
11. Konseglu, Y., Kavas, H., Aktas, B.: Surface effects on magnetic properties of superparamagnetic nanoparticles. *Phys. Status Solidi A* **203**, 1595–1601 (2006)
12. Hummers Jr W.S., Offeman R.E.: Preparation of graphitic oxide. *J. Am. Chem. Soc.* **80**(6), 1339–1339 (1958)
13. Krishnamoorthy, K., Veerapandian, M., Yun, K., Kim, S.-J.: The chemical and structural analysis of graphene oxide with different degrees of oxidation. *CARBON* **53**, 38–49 (2013)
14. Ali, R., Mahmood, A.: Muhammad Azhar Khan. Adeel Hussain Chughtai, Muhammad Shahid, Imran Shakir, Muhammad Farooq Warsi, *Journal of Alloys and compounds* **584**, 363–368 (2014)
15. Sumangala, T.P., Mahender, C., Sahu, B.N., Venkataramani, N.: Shiva Prasad, Study of magnesium ferrite nanoparticles with excess iron content. *Phys. B* **448**, 312–315 (2014)
16. Khurana, G., Kumar, N., Kooriyattil, S., Katiyar, R.S.: Structural, magnetic, and dielectric properties of graphene oxide/Zn x Fe1– x Fe₂O₄ composites. *J. Appl. Phys.* **117**(17), 17E106 (2015)
17. Ameer, S.: Iftikhar Hussain Gul, Nasir Mahmood, Muhammad Mujahid, Semiconductor-to-metallic flipping in a ZnFe₂O₄–graphene based smart nano-system: temperature/microwave magneto-dielectric spectroscopy. *Mater. Charact.* **99**, 254–265 (2015)
18. Muhammad Ajmal, M.U.: Islam, Absar Ali, Structural, Electrical and dielectric properties of hexa- ferrite-polyaniline nano-composites. *J. Supercond. Nov. Magn.* **31**, 1375–1382 (2018)
19. Mohsin Saeed, M., Ajmal, M., Islam, M. U., Aamir Nazir, M.: Synthesis and characterization of Y-type ferrite reinforced graphene oxide composites. *J. Supercond. Nov. Magn.* **33**, 2705–2713 (2020)
20. Waqas Nafees, M., Islam, M. U., Ajmal, M., Hussain, M.: Aisha Iftikhar and Shahzad Naseem, Effect of Al³⁺ substitution on the electrical and magnetic properties of Li-base ferrites. *Mater. Res. Exp.* **6**(12), 126121 (2019)
21. Rana, M.U., Islam, M.U., Ahmad, I., Abbas, T.: Determination of Magnetic properties and Y-K angles in Cu-Zn-Fe-O system. *J. of Mang. and Mag. Mat.* **187**(2), 242–246 (1998)
22. Smit, J., Wijn, H.P.J.: Ferrites, Philips Technical Library, Eindhoven, 150 (1959)
23. Saravanan, M., Sabari Girisun, T.C.: Enhanced nonlinear optical absorption and optical limiting properties of superparamagnetic spinel zinc ferrite decorated reduced graphene oxide nanostructures. *Appl. Surf. Sci.* **392**, 904–911 (2017)
24. Ali, I., Shakoor, A.: M U Islam, Muhammad Saeed, Synthesis and characterization of hexagonal ferrite Co₂Sr₂Fe₁₂O₂₂ with doped polypyrrole composites. *Curr. Appl. Phys.* **13**(6), 1090–1095 (2013)

Publisher's Note Springer Nature remains neutral with regard to jurisdictional claims in published maps and institutional affiliations.